RESEARCH ARTICLE

THBS1 mediates hypoxia driven EndMT in pulmonary hypertension

Bingming Peng[1,2,3] | **Yingzhen Zhou**[1,2,3] | **Xingmeng Fu**[1,2,3] | **Li Chen**[1,2,3] | **Zhengxia Pan**[1,2,3] | **Qijian Yi**[1,2,3] | **Tengteng Zhao**[4] | **Zhou Fu**[1,2,3] | **Ting Wang**[1,2,3,4] (ID)

[1]Department of Respiratory, Thoracic and Cardiac Surgery, Cardiovascular Medicine, Children's Hospital of Chongqing Medical University, National Clinical Research Center for Child Health and Disorders, Ministry of Education Key Laboratory of Child Development and Disorders, Chongqing, China

[2]China International Science and Technology Cooperation Base of Child development and Critical Disorders, Children's Hospital of Chongqing Medical University, Chongqing, China

[3]Chongqing Engineering Research Center of Stem Cell Therapy, Children's Hospital of Chongqing Medical University, Chongqing, China

[4]Department of Medicine, Section of Physiology, Division of Pulmonary, Critical Care and Sleep Medicine, University of California, San Diego, La Jolla, California, USA

Correspondence
Ting Wang, Department of Respiratory, Children's Hospital of Chongqing Medical University, Chongqing 400014, China.
Email: wangting@zqykdxfsetyy1. wecom.work

Abstract

Long-term hypoxia is one of the main causes of pulmonary vascular remodeling in pulmonary hypertension (PH) associated with congenital heart disease (CHD) children. Endothelial to mesenchymal transition (EndMT) is an important pathological basis of pulmonary vascular remodeling in PH. We observed that Fibronectin 1 (FN1) had strong protein–protein interactions with both Thrombospondin 1 (THBS1) and Transglutaminase 2 (TGM2) in PH with venous peripheral bloods samples from pediatric patients and healthy children. LungMAP CellCards and heatmaps of human PAEC in PH patients and lung tissues in hypoxia induced PH mice model were used to show that THBS1 and FN1 were significantly elevated. We studied the relationship between THBS1 and FN1 in vivo, by using SUHX-induced PH mice model, and in vitro, by using hypoxia-induced human PAEC. The results showed that hypoxia could result in EndMT and inhibiting THBS1 could reverse EndMT in vivo and in vitro, verifying our transcriptome results. Taken together, our

Abbreviations: BPD, bronchopulmonary dysplasia; CHD, congenital heart disease; DEG, differential expression genes; EC, endothelial cell; ECM, Endothelial Cell Medium; ECM, extracellular matrix; EndMT, endothelial to mesenchymal transition; FN1, Fibronectin 1; HPAEC, human pulmonary arterial endothelial cell; HUVEC, human umbilical vein endothelial cell; LVEC, lung vascular endothelial cell; mPAP, mean pulmonary arterial pressure; PASP, pulmonary artery systolic pressure; PH, pulmonary hypertension; PMVEC, pulmonary microvascular endothelial cell; RHC, right heart catheterization; RV, right ventricle; RVP, right ventricle pressure; RVSP, right ventricular systolic pressure; siRNA, small interfering RNA; TBS, Tris-buffered saline; TGF-β, transforming growth factor-β1; THBS1, TSP1, Thrombospondin 1; TTE, transthoracic echocardiography; VE-cad, vascular endothelial cadherin; α-SMA, alpha smooth muscle actin.

research demonstrated that THBS1 could mediate hypoxia driven EndMT of PH, providing a new insight of research in the pathophysiology of PH.

KEYWORDS

EndMT, hypoxia, pulmonary hypertension, pulmonary vascular remodeling, THBS1

INTRODUCTION

Pulmonary hypertension (PH), symbolized by pulmonary vascular remodeling with endothelial cells (ECs) dysfunction,[1] is a typical complication of congenital heart disease (CHD), which eventually leads to right heart failure and significantly increases morbidity and mortality in pediatric patients.[2] Long-term hypoxia is one of the major causes contributing to pulmonary vascular remodeling in CHD-PH children.[3] Hypoxia triggers the endothelial to mesenchymal transition (EndMT) during pulmonary vascular remodeling.[4]

EndMT, which is a biological process in ECs which progressively change their endothelial phenotype into a mesenchymal or myofibroblastic phenotype,[5] Constitutes a significant pathological foundation for pulmonary vascular remodeling in PH.[5–7] The migration involved in EndMT begins with the disruption of cell–cell interactions facilitated by membrane proteins like vascular endothelial cadherin (VE-cad) and CD31. Then, the cells undergo a gradual loss of distinct endothelial markers and begin to express mesenchymal markers such as alpha smooth muscle actin (α-SMA), Fibronectin 1 (FN1), and vimentin.[8,9] Previous research has found that hypoxia promotes EndMT in human umbilical vein endothelial cells (HUVECs), as well as in human and rat ECs.[10–12]

FN1, which is also one of the mesenchymal markers, is located across the cell surface and extracellular matrix (ECM) in the character of dimers or multimers, which is playing a role in cell adhesion and migration processes implicated in tumor metastasis.[13] It is reported that FN1 increased in a rat model of PH induced by hypoxia,[14] demonstrated that hypoxia has the potential to trigger EndMT in PAH. However, the mechanism of hypoxia induced EndMT is still not clear.

The secreted matricellular protein thrombospondin 1 (THBS1, also called TSP1) is recognized to play a pivotal role in vascular health as well as the process of vascular disease.[15] Research revealed that mice lacking THBS1 were shielded from hypoxia-induced PH,[16,17] and the expression of THBS1 was increased in lung tissues from PH patients compared with non-PH controls.[16,18,19] Meanwhile, THBS1 was reported to be regulated by HIF-2α in hypoxia-driven vascular remodeling of PH.[20]

In this study, we hypothesize that THBS1 is associated with hypoxia driven EndMT of PH. Herein, we focused on the relationship between THBS1 and FN1 in vivo, by using SUHX-induced PH mice model, and in vitro, by using hypoxia-induced human PAEC. Collectively, these studies offer new mechanistic insights into the THBS1 involved hypoxia induced EndMT and its contribution to PH.

METHODS

Ethical approval

Ethical approval was approved by the Children's Hospital of Chongqing Medical University, and all patients' families were informed and signed informed consent forms. The ethics committee approval number is:(2022) Ethics Review (Research) No.[8] This study was approved by the Ethics Committee of the University of California, San Diego (La Jolla, CA) and executed according to the IACUC guidelines. Following successful model identification, the mice were euthanized by dislocation following intraperitoneal injection of pentobarbital sodium anesthesia. The lung tissue of the mice was then collected for experimental analysis. The use of neck breaking after pentobarbital sodium anesthesia ensures a painless and rapid death, meeting the criteria for euthanasia. Animal remains were carefully packaged in opaque infectious special plastic bags, stored in the animal center's freezer, and handled by the Animal Center.

Recruitment of pediatric participants

A study with a total of 153 participants, aged 11 years old, was conducted. This included 55 patients initially diagnosed with PH, 55 patients with CHD, and 43 reference subjects. The detailed baseline characteristics can be found in Table 1. Patients with CHD and pulmonary arterial hypertension (PAH) were diagnosed using transthoracic echocardiography (TTE) administered by a skilled sonographer. In patients, PAH was characterized by a pulmonary artery systolic pressure (PASP) exceeding 35 mmHg. PASP was determined using Doppler TTE to calculate the

TABLE 1 Personal features of participants.

Characteristic	CHD-PH $n = 55$	CHD $n = 55$	Healthy control $n = 43$	p Value
Sex (n, %)				0.723
Female	37 (67.3%)	39 (70.9%)	27 (57.4%)	
Male	18 (32.7%)	16 (29.1%)	16 (42.6%)	
Age (month)	30.4 ± 29.2	31.7 ± 19.9		0.098
Delivery mode (n, %)				0.544
Vaginal birth	20	19		
Cesarean delivery	35	36		
Feeding mode (n, %)				0.383
Breastfeeding	33 (60%)	36 (65.5%)		
Artificial formula feeding	8 (14.5%)	6 (10.9%)		
Combined	14 (25.5%)	13 (23.6%)		
Diagnosis[a] (n)				
Atrial septal defect	27	23		
Anomalous pulmonary venous connection	2	6		
Pulmonary stenosis	0	4		
Patent ductus arteriosus	19	20		
Tetralogy of Fallot	0	1		
Ventricular septal defect	17	21		
Coronary arteriovenous fistulas	0	1		
Double outlet right ventricle	0	1		
PASP (mmHg)	55.9 ± 13.1			
Severity of PH (n, %)				
Mild	28 (50.9%)			
Moderate	24 (43.6%)			
Severe	3 (5.5%)			

Note: PS. Methods: One-way ANOVA test for normally distributed data (shown as mean ± SD), and χ^2 test for nonnormally distributed data (shown as number).

[a]Patients may have more than 1 type of congenital heart disease.

gradient between right ventricular and right atrial pressures during systole. The simplified Bernoulli equation was employed to evaluate the velocity within the tricuspid regurgitation jet (PASP = 4 × [tricuspid regurgitation]2 + mean right atrial pressure). At the same time, 43 healthy children without respiratory symptoms, abnormalities on chest X-rays, or known lung diseases were included. Participants were excluded if they met any of the following criteria: (1) history of surgery before CHD diagnosis; (2) premature or test tube birth; (3) use of oral/nasal corticosteroids or antibiotics within 4 weeks before enrollment; (4) use of immunosuppressive medications; (5) oral or pulmonary infection within 4 weeks before enrollment; and (6) known conditions linked to PH, such as autoimmune diseases, liver and renal disorders, and hematologic conditions. The study was approved by the ethics committee of Children's Hospital Affiliated to Chongqing Medical University and adhered to the Declaration of Helsinki. Written informed consent was obtained from all parents or legal guardians of the pediatric participants.

Collection of peripheral blood

Venous Peripheral bloods were gathered on the same day as TTE was conducted for patients by collecting the venous peripheral blood with an anticoagulant EDTA tube to draw at least 6 mL, then mix up and down after drawing blood. Anticoagulant blood was centrifuged at 3000 rpm, 10 min, 450 g, 4°. Aspirate the light-yellow supernatant, which is plasma, and dispense them into 1.5 mL RNase-free EP tubes. Precipitation was added Trizol in a ratio of 1:3 or 1:6 and mix well. After that, precipitation was aliquoted into 15 mL sized EP tubes. The samples were preserved at −80°C until further processing, which occurred within a span of 2 weeks.

Experimental animals

Male mice, aged 8 weeks and weighing 25 g, were employed for in vivo experiments to assess pulmonary hemodynamics. The study protocols and animal care practices received approval from the Institutional Animal Care and Use Committee (IACUC) at the University of California, San Diego (La Jolla, CA), and adhered to IACUC guidelines in line with national and international regulations. The mice were housed in standard cages with a 12-h light-dark cycle, and they had ad libitum access to food and tap water.

To induce experimental PH, mice were exposed to normobaric hypoxic conditions using hypoxic chambers (Cat. No. A30271-P; BioSpherix) filled with a hypoxic gas mixture (10% O_2 in N_2) for a duration of 6 weeks. Additionally, the mice received intraperitoneal injections of Sugen at a dose of 20 mg/kg (Sigma) once a week. The hypoxic chamber, measuring 30 inches wide, 20 inches deep, and 20 inches high, was equipped with an O_2 sensor (Cat. No. ProOx P110-E702) for continuous monitoring of O_2 concentration and partial pressure of O_2 (PO_2) within the chamber. The normoxic control group of mice was housed in the same animal facility under room air conditions (21% O_2). The mice's feed, bedding, and water were changed weekly.

Following hypoxic exposure, the mice were anesthetized through continuous inhalation of isoflurane (1.5%), following which right heart catheterization (RHC) was performed to assess right ventricle pressure (RVP) and right ventricle (RV) contractility (RV-±dP/dt). This was done using a pressure transducer catheter (Millar Instruments, PVR1030) inserted into the RV via the external right jugular vein. Before each measurement, the catheter underwent baseline calibration to ensure a zero basal pressure. The recorded RVP and RV-±dP/dt data were analyzed using AD Instruments Lab Chart software.

The mean pulmonary arterial pressure (mPAP) was calculated from the right ventricular systolic pressure (RVSP) using the equation: mPAP (in mmHg) = 0.61 RVSP + 2.[21,22] Meanwhile, some mice, which do not experience RVSP test, were killed and then lung tissues were sectioned (4 μm thick) and subjected to hematoxylin–eosin staining.

Pulmonary arterial endothelial cells from humans (HPAECs) at passages 3–6 were obtained from ScienCell Research Laboratories, and cultured in complete Endothelial Cell Medium (ECM). The cells were kept in a CO_2 incubator (5%, Thermo) at 37°C and utilized for experiments when they reached 80%–90% confluence.

Human pulmonary arterial endothelial cells (HPAECs) were transfected with either control small interfering RNA (siRNA) (siNT) or siRNA targeting THBS1 using the RNAiMax transfection reagent (Cat. No. 13778075; Invitrogen) for a duration of 72 h. Subsequently, the transfected cells were incubated in medium containing 10% fetal bovine serum (FBS) for 48 h. siTHBS1 sense strand: GCGUGAAGUGUACUAGCUATT, and antisense strand: UAGCUAGUACACUUCACGCTT.

Real-time RT-PCR

The total RNA extracted from lung tissues and cells underwent purification, followed by cDNA synthesis using a PrimeScript RT Reagent Kit from Takara. PCR reactions, detailed in the Supporting Information, were carried out using Real MasterMix (SYBR Green; Tiangen). The expression levels were normalized using β-actin as an internal control to calculate relative expression. The details of the primers are provided in the Supporting Information.

Western blot analysis

HPAECs were rinsed with ice-cold PBS and then suspended in 1X RIPA buffer (Millipore) supplemented with a protease inhibitor cocktail tablet (Roche). The cell lysates were centrifuged at 12,000 g for 15 min, and the resulting supernatant was collected. Protein concentrations were quantified using a Nano-Drop spectrophotometer (Thermo Fisher Scientific). The samples were loaded onto an 8% SDS-PAGE gel, and the proteins were electroblotted onto nitrocellulose membranes. These membranes were blocked in 5% bovine serum albumin in 1X Tris-buffered saline (TBS) containing 0.1% Tween 20 for 1 h at room temperature. Subsequently, they were incubated overnight at 4°C with primary antibodies targeting THBS1 (Cat. No. 37879S, 1:1000; Cell
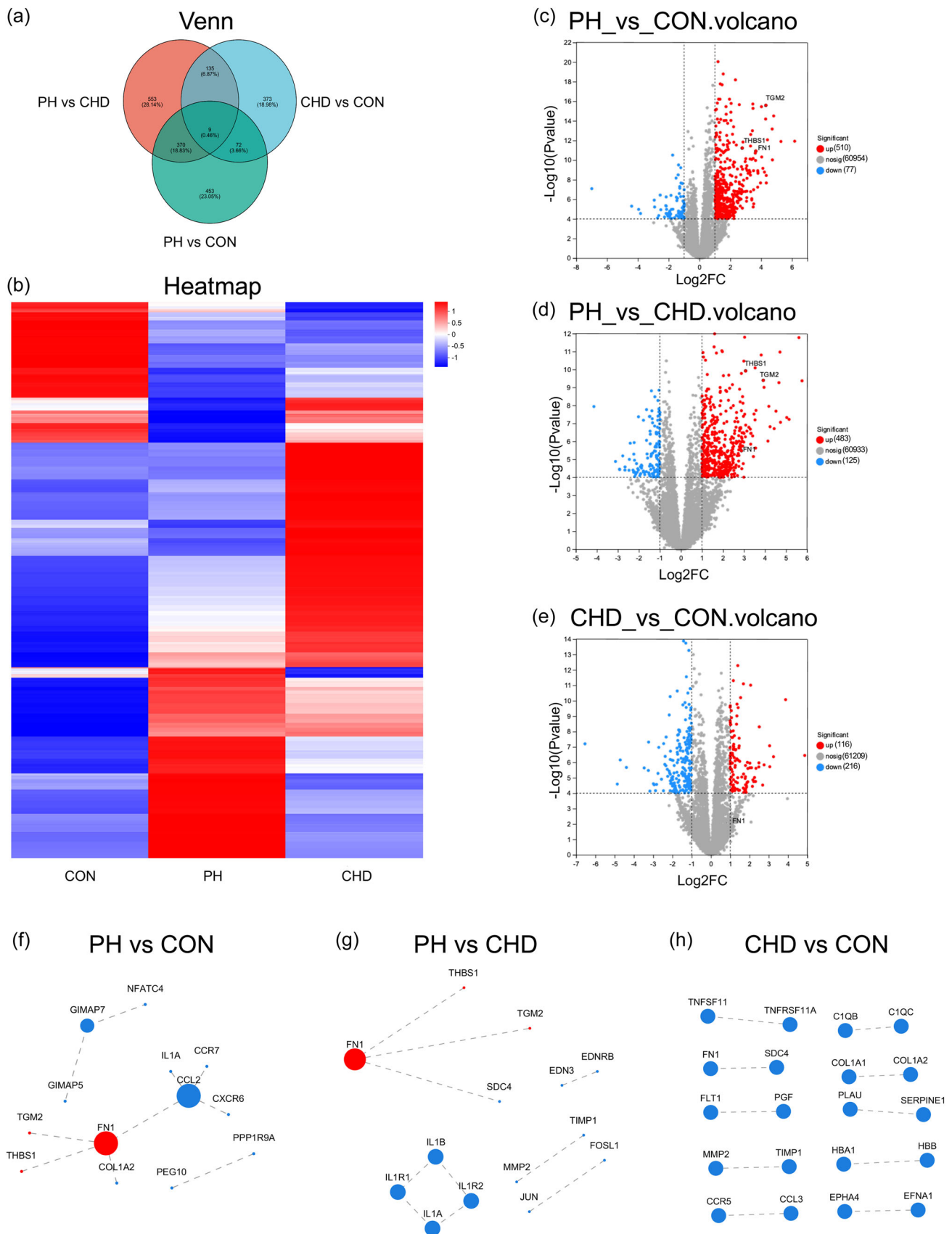
FIGURE 1 (See caption on next page).

Signaling Technology), FN1 (Cat. No. 26836S, 1:1000; Cell Signaling Technology), CD31 (Cat. No. 77699S, 1:1000; Cell Signaling Technology), VE-cad (Cat. No. 2500S, 1:1000; Cell Signaling Technology), vimentin (Cat. No.5741S, 1:1000; Cell Signaling Technology), and b-actin (Cat. No. sc-47778; 1:2000; Santa Cruz Biotechnology; as a loading control). The membranes were then exposed to anti-mouse (Cat. No. 7076S; Cell Signaling Technology) or anti-rabbit (Cat. no. 7074S; Cell Signaling) secondary antibodies for 1 h at room temperature the following day. Blots were developed using ECL Prime Western blot analysis Detection Reagents (GE Healthcare), and the bands were visualized using ImageJ software.

Statistical analysis

To determine the differentially expressed genes (DEGs) between two distinct samples, the expression level of each transcript was assessed using the transcripts per million reads (TPM) method. Gene abundances were quantified using RSEM (http://deweylab.biostat.wisc.edu/rsem/). The analysis of differential expression was conducted using DESeq. 2, DEGseq, or EdgeR with a Q value of ≤0.05. Genes with a |log2FC| > 1 and a Q value of ≤0.05 (for DESeq. 2 or EdgeR) or a Q value of ≤0.001 (for DEGseq) were considered significantly differentially expressed genes. The experimental data are presented as the mean ± standard error of the mean (SEM). Statistical analyses were performed using Prism 5.0 software (GraphPad). Two-way analysis of variance (ANOVA) was used to assess significant differences in the variables across different groups. In case of a significant overall test result, Tukey's test was utilized for pairwise comparisons between specific groups. A significance level of $p < 0.05$ was considered statistically significant. Each experiment was repeated at least three times, yielding consistent results.

Full details of transcriptome procedures, which including the process included RNA extraction, library preparation, and sequencing using Illumina HiSeq X Ten or NovaSeq. 6000 platforms, followed by read mapping, differential expression analysis, functional enrichment analysis, and identification of alternative splice events identification are provided in the Supporting Information.

RESULT

Characterization of participants in three cohorts

Venous peripheral blood samples were collected from 55 patients with coronary heart disease (CHD), 55 patients with PH, and 43 healthy control subjects, based on the established inclusion and exclusion criteria. As shown in Table 1, there were no statistically significant differences in sex or mode of delivery among the PH, CHD, and control groups.

Differential gene expression analysis of the transcriptome in three groups

A total of 1219.21 Gb Clean Data was obtained and cleaned to ensure each sample reach more than 6.02 Gb through the transcriptome analysis of 168 samples while the percentage of Q30 bases was more than 93.4%. A total of 43,277 expressed genes were detected in this analysis, of which 42,420 known genes. The reference gene source is Homo_sapiens and reference genome version is GRCh38.p13.

To further analyze the differential genes between the three groups, we established three differential gene sets between the groups, namely PH versus CON, PH versus CHD and CHD versus CON. Venn analysis of differential gene sets between groups were showed in Figure 1a. A total of 370 identical genes were identified between PH versus CON and PH versus CHD gene sets, suggesting that these 370 genes may be the key gene sets. The

FIGURE 1 Transcriptomic analysis in the CHD group, pulmonary artery hypertension associated with CHD (PH) group, and pediatric controls. (a) Venn analysis of differential gene sets between groups. (b) Heat map of cluster analysis of differential genes among three groups. Red represents higher expression gene and blue represents lower expression genes. Volcano plot of differential genes of PH versus CON gene sets (c), PH versus CHD gene sets (d) and CHD versus CON gene sets (e). Red dots represent significantly upregulated genes, blue dots represent significantly downregulated genes, and gray points are nonsignificantly different genes. Differential gene–protein interaction network analysis (10 groups) of PH versus CON group (f), PH versus CHD group (g), and CHD versus CON group (h). Nodes represent genes, and edges represent the interaction between the two genes. The size of a node is proportional to the degree of the node. CHD, congenital heart disease; CON, healthy children; PH, Pulmonary hypertension associated with congenital heart disease. CHD versus CON, differential gene sets between CHD and CON group; PH versus CHD, differential gene sets between PH and CHD group; PH versus CON, differential gene sets between PH and CON group. *$p < 0.05$, **$p < 0.01$.
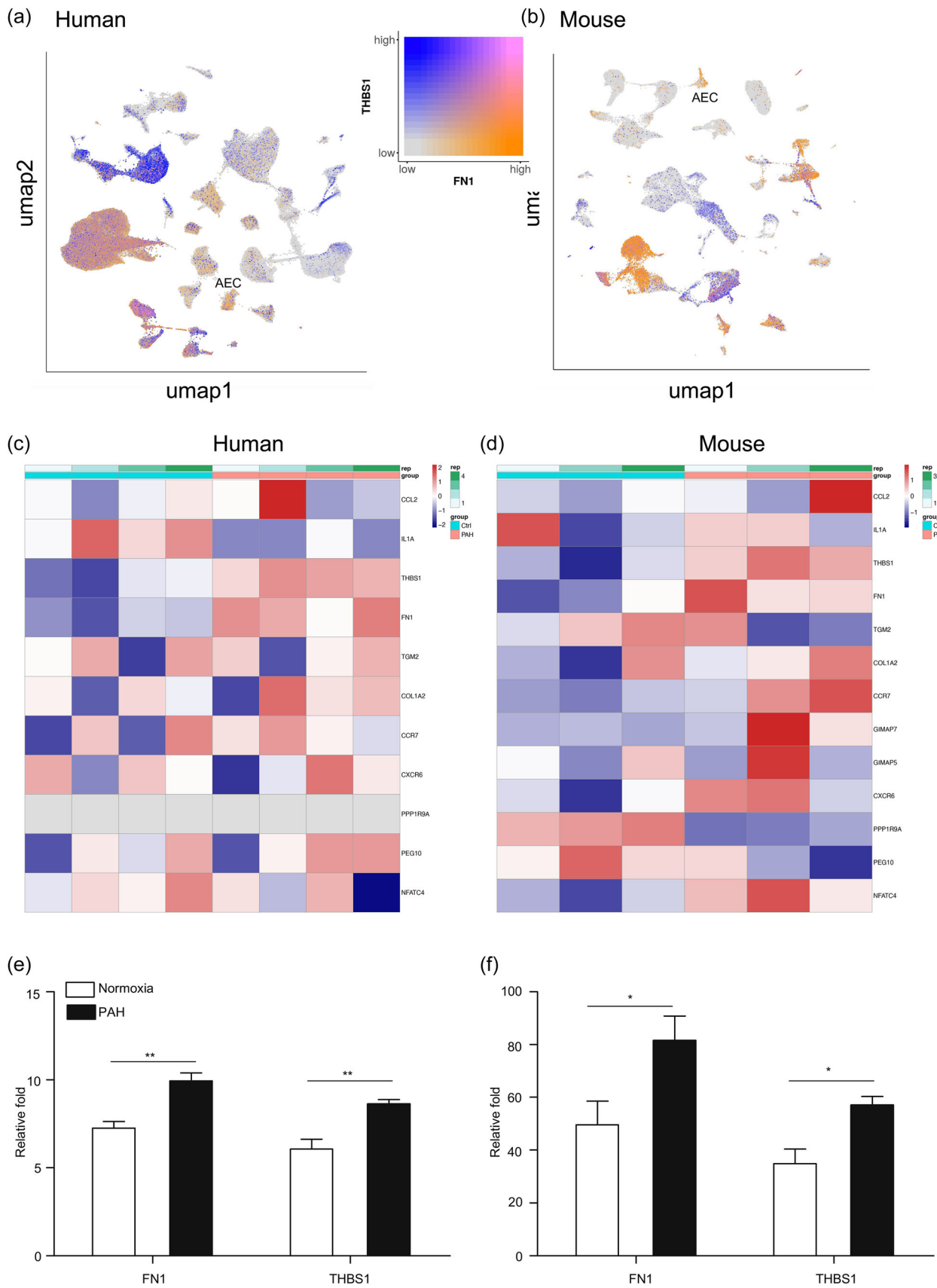
FIGURE 2 (See caption on next page).

significantly DEGs (-logFC- >1, p value < 0.05) were visualized using heatmaps representations (Figure 1b).

THBS1 and FN1 significantly increased in PH group

Volcano plots were employed to visually depict the differentially expressed genes between groups to further understand the differences in gene expression, and it was found that THBS1, FN1 and TGM2 were significantly elevated in PH versus CON (Figure 1c) and PH versus CHD (Figure 1d) gene sets compared with CHD versus CON (Figure 1e) gene sets, indicating that these three genes may be the key genes in PH group. To further study whether there is an interaction between gene products and proteins, protein interaction network analysis ranked the top 10 protein interactomes, and it was showed that FN1 had strong protein–protein interactions with both THBS1 and TGM2 in PH versus CON (Figure 1f) and PH versus CHD (Figure 1g) gene sets compared with CHD versus CON (Figure 1h).

THBS1 and FN1 were highly expressed in PH patients and hypoxia-induced PH mice model

Meanwhile, we also interested in investigating THBS1 and FN1 expression of human and mice PH model. GSE168905 and GSE110131 databases were found to show the RNA-seq data of human PAEC in PH patients (Figure 2a) and lung tissues in hypoxia induced PH mice model (Figure 2b), respectively. After quantifying the results of Figure 2a,b, we found that THBS1 and FN1 genes both had a statistical difference of human ($p < 0.01$) (Figure 2c) and mice ($p < 0.05$) (Figure 2d) PAH group compared with their control group. Since LungMAP CellCards displayed single-cell transcriptomic datasets of 104 human lungs and 17 mouse lung normal samples,[23] we utilized it to investigate THBS1, FN1 and TGM2 expression in PAEC and it was found that THBS1 and FN1 were expressed in human (Figure 2e) and mice (Figure 2f) PAEC.

Inhibiting THBS1 attenuates SUHX-induced EndMT in PH mice model and hypoxia-induced EndMT in HPAEC

To further explore the relationship between FN1 and THBS1 in PH, SUHX-induced mice PH model and hypoxia-induced PH in HPAEC were both established. Figure 3a showed the experimental protocol (Figure 3a), RVSP (Figure 3b), and H&E staining (Figure 3c) were conducted to identify the PH mice model. The results showed that LSKL, the inhibitor of THBS1, could reduce the RVSP and peripulmonary artery inflammatory response.

We then used western blot to explore the function of THBS1 in EndMT of PH by using hypoxia induced HPAEC cell line and SUHX-induced PH mice model. In vivo, the results demonstrated that SuHx could induce EndMT, which displayed as significantly increased expression of FN1 and vimentin, which were mesenchymal cell markers, and decreased expression of CD31 and VE-cad, which were EC markers (Figure 4a–f). We also found that inhibition of THBS1 could reduce SUHX-induced EndMT, suggesting that THBS1 was involved in hypoxia-induced EndMT of PH mice model. In vitro, siRNA was used to knockdown THBS1 gene, and the results showed the similar trend. Knockdown of THBS1 also reduced hypoxia induced EndMT in HPAEC (Figure 5a–f). Above all, THBS1 was involved in hypoxia induced EndMT of PH in vivo and in vitro.

DISCUSSION

Here, we used venous peripheral bloods samples from pediatric patients and healthy children to explore transcriptomic differential genes of PH by using Venn analysis and heatmap. Protein interaction network analysis was employed to rank the top 10 protein interactomes and it was showed that FN1 had strong protein–protein interactions with both THBS1 and TGM2 in PH. Then, LungMAP CellCards and heatmaps of human PAEC in PH patients and lung tissues in hypoxia induced PH mice model were used to show that THBS1 and FN1 were significantly elevated. Next, we studied the relationship

FIGURE 2 THBS1 and FN1 were highly expressed in PH patients and hypoxia-induced PH mice model. Heatmap of key differential genes in pulmonary AEC line from healthy group and pediatric PH patients (a), mouse hypoxia-induced PH model and control group (b). (c) and (d) represent the quantitative results of THBS1 and FN1 gene expression in (a) and (b), respectively. Expression of THBS1 and FN1 genes in the lung endothelial cells (AEC) in human lung (e) and mouse lung (f) from LungMAP CellCards. The data in (a) and (b) are from databases GSE168905 and GSE110131. PH in (a), idiopathic pulmonary hypertension patients. PH in (b), hypoxia induced pulmonary hypertension. AEC, artery endothelial cells; Ctrl, control group. *$p < 0.05$, **$p < 0.01$.
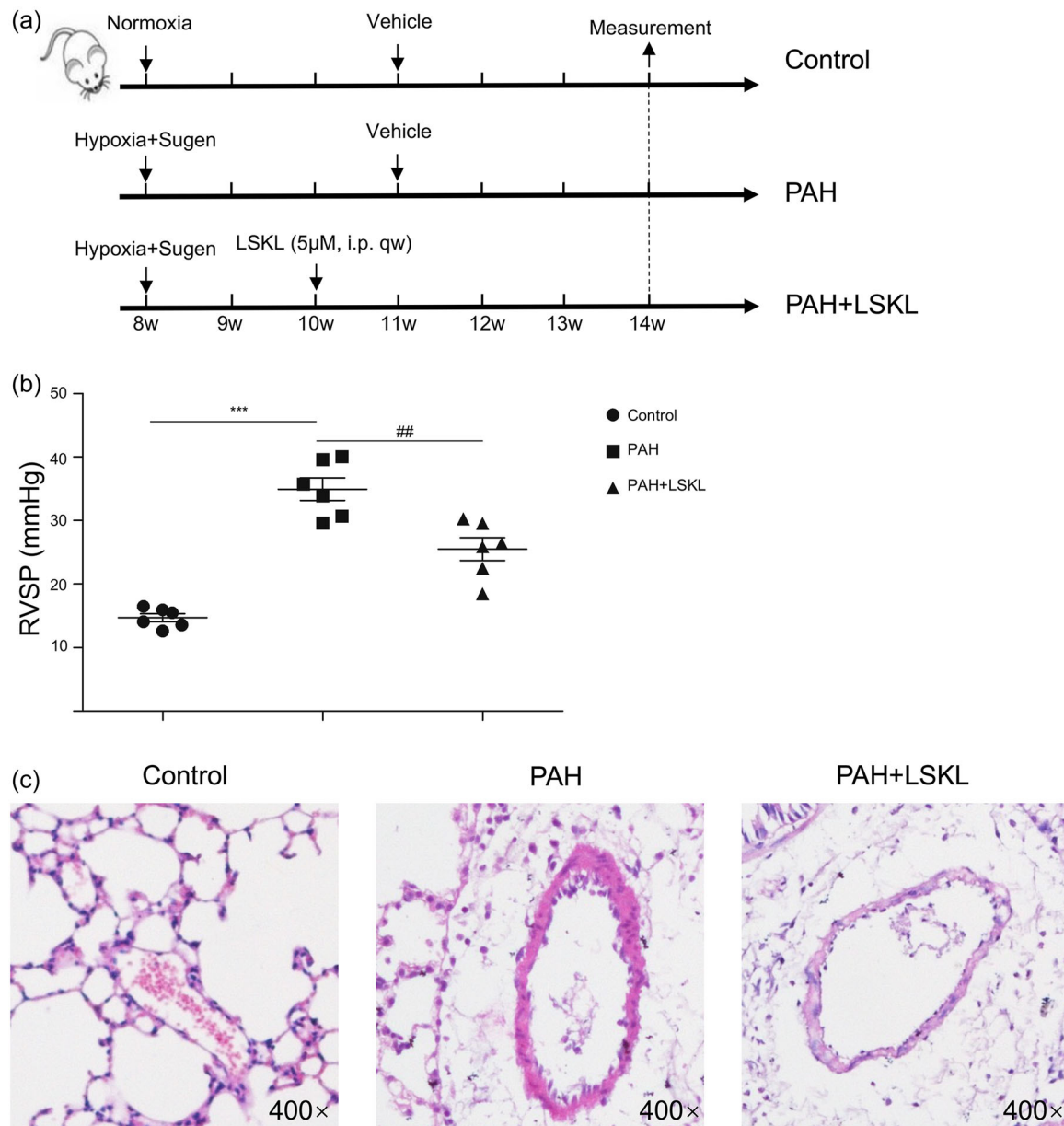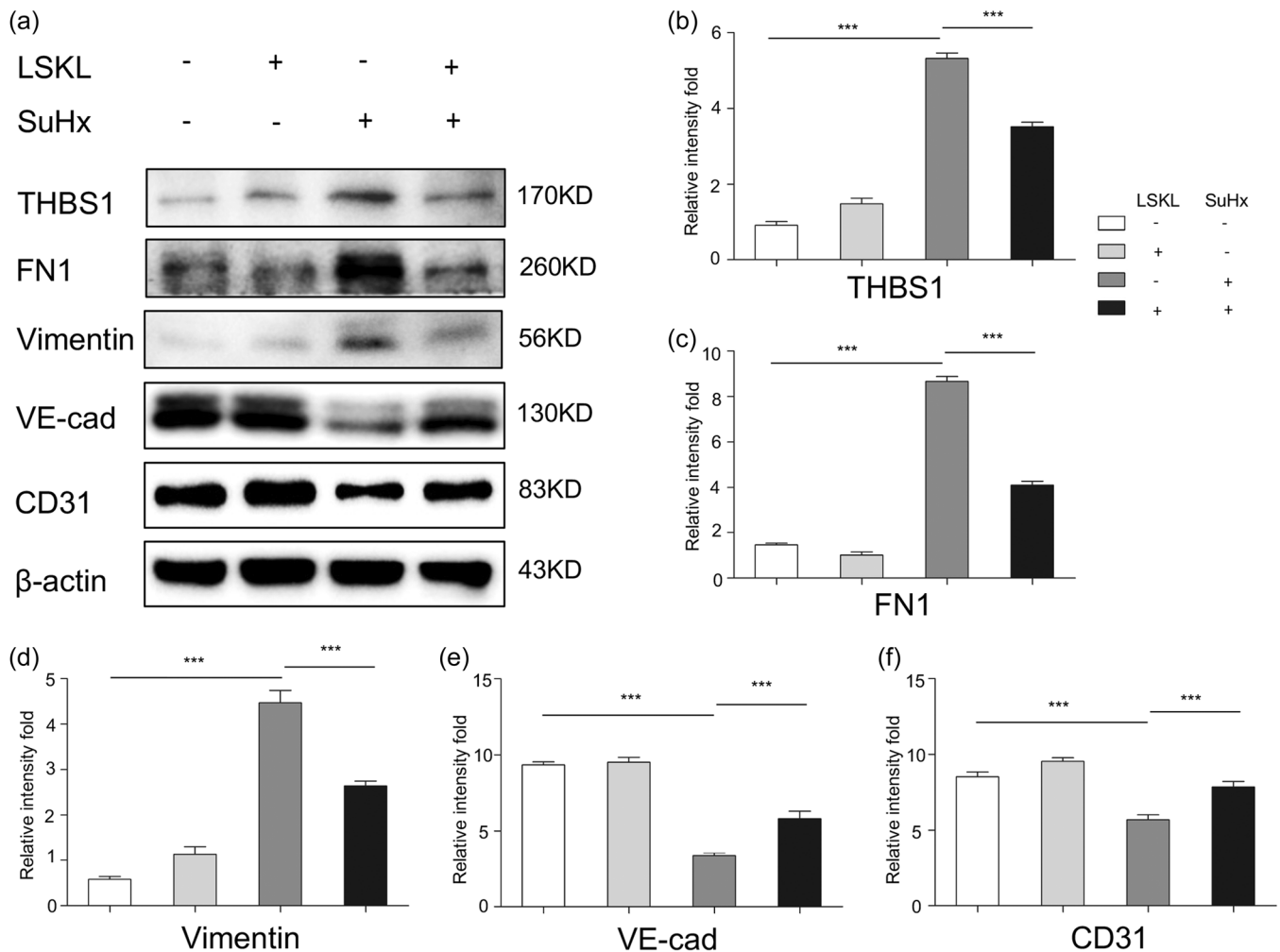
FIGURE 3 Inhibiting THBS1 alleviates SuHx-induced pulmonary hypertension model. (a) Eight-week-old C57Bl/6 mice are subjected to normoxia (Control) or hypoxia (10% O_2) + Sugen-5416 for 6 weeks. LSKL (5 μM/per mouse/week) was intraperitoneally injected (ip) at the third week of hypoxia exposure and continuously injected for 4 weeks during hypoxia. (b) Right ventricular systolic pressure (RVSP), estimated mean pulmonary arterial pressure (mPAP), RV-þ(dP/dt)max, RV contractility index [RV-þ(dP/dt)max/RVSP] and heart rate in control ($n = 6$), PH ($n = 6$), and PH + LSKL ($n = 6$) mice. ***$p < 0.001$ versus Control; ##$p < 0.01$ versus PH + LSKL (ANOVA). (c) Hematoxylin–eosin staining of the lung tissues in control ($n = 6$), PH ($n = 6$), and PH + LSKL ($n = 6$) mice. CON, C57 B1/6 mice; LSKL, inhibitor of THBS1; PH, Sugen-5416 plus hypoxia [SuHx] induced pulmonary hypertension.

between THBS1 and FN1 in vivo, by using SUHX-induced PH mice model, and in vitro, by using hypoxia-induced human PAEC. Western blot was used to analysis the role of THBS1 in EndMT of PH and the result showed that hypoxia could result in EndMT, performed as increased expression of FN1 and vimentin, which were mesenchymal cell markers, and decreased expression of CD31 and VE-cad, which were EC markers. However,

inhibiting THBS1 could reverse EndMT, indicating that THBS1 may participate in hypoxia driven EndMT of PH. The discovery of THBS1 as a potential marker for PH in children is of paramount importance.

Most of the pediatric CHD patients undergo a long-term hypoxia due to left to right shunt and may lead to PH at the end of course,[24] suggesting that hypoxia may play a crucial role in the pathological changes of

FIGURE 4 Inhibiting THBS1 attenuates SUHX-induced EndMT in PH mice model. (a) Western blot analysis shows THBS1(Thrombospondin 1), FN (fibronectin) 1, CD31, VE (vascular endothelial)-cadherin, and vimentin protein expression levels in lung tissues from SuHx-PH models. (b–f) Graphs show the quantification of THBS1, FN1, CD31, VE-cad, and vimentin protein expression levels normalized by β-actin protein expression measured from SuHx-PH models. Error bars represent means ± SEM ($n = 6$ in each group). *$p < 0.05$, **$p < 0.01$, and ***$p < 0.001$. LSKL, inhibitor of THBS1; VE-cad, VE-cadherin.

pulmonary vascular remodeling of PH. It is reported that hypoxia could induce EndMT in pulmonary vascular remodeling of chronic hypoxia induced PH rats, in lung vascular endothelial cells (LVECs) isolated from IPAH patients and in hypoxia induced pulmonary micro-vascular endothelial cells (PMVECs).[4,25] We also demonstrated that hypoxia could induce increased expression of FN1 and vimentin, which were mesenchymal cell markers, and decreased expression of CD31 and VE-cad in vivo, by using SUHX-induced PH mice model, and in vitro, by using hypoxia-induced human PAEC. Our results showed increased expression of THBS1 together with hypoxia induced EndMT. This result consisted with previous research which showed that THBS1 increased in lungs from PH patients[19] and induction of THBS1 could mimic hypoxia in hypoxic murine and human lungs.[20]

We also found that in vivo, inhibition of THBS1 could reduce SUHX-induced EndMT, suggesting that THBS1 was involved in hypoxia-induced EndMT of PH mice model. In vitro, siRNA was used to knockdown THBS1 gene, and the results showed that knockdown of THBS1 reduced hypoxia induced EndMT in HPAEC. It is reported that TSP-1 could bind to the TGF-β small latent complex which comprised of the N-terminal latency associated peptide (LAP) and the C-terminal mature domain through its type 1 repeats.[26] TSP-1/TGF-β pathway plays a certain role in the pathogenesis of diabetes, liver fibrosis, multiple myeloma fibrosis and other diseases.[27–29] It was shown that THBS1$^{-/-}$ mice were protected from hypoxia-induced PH,[30] confirming our result. Additionally, it has been demonstrated that THBS1 activates transforming growth factor-β1 (TGF-β1) with increased Rho-kinase signaling in hypoxia-exposed
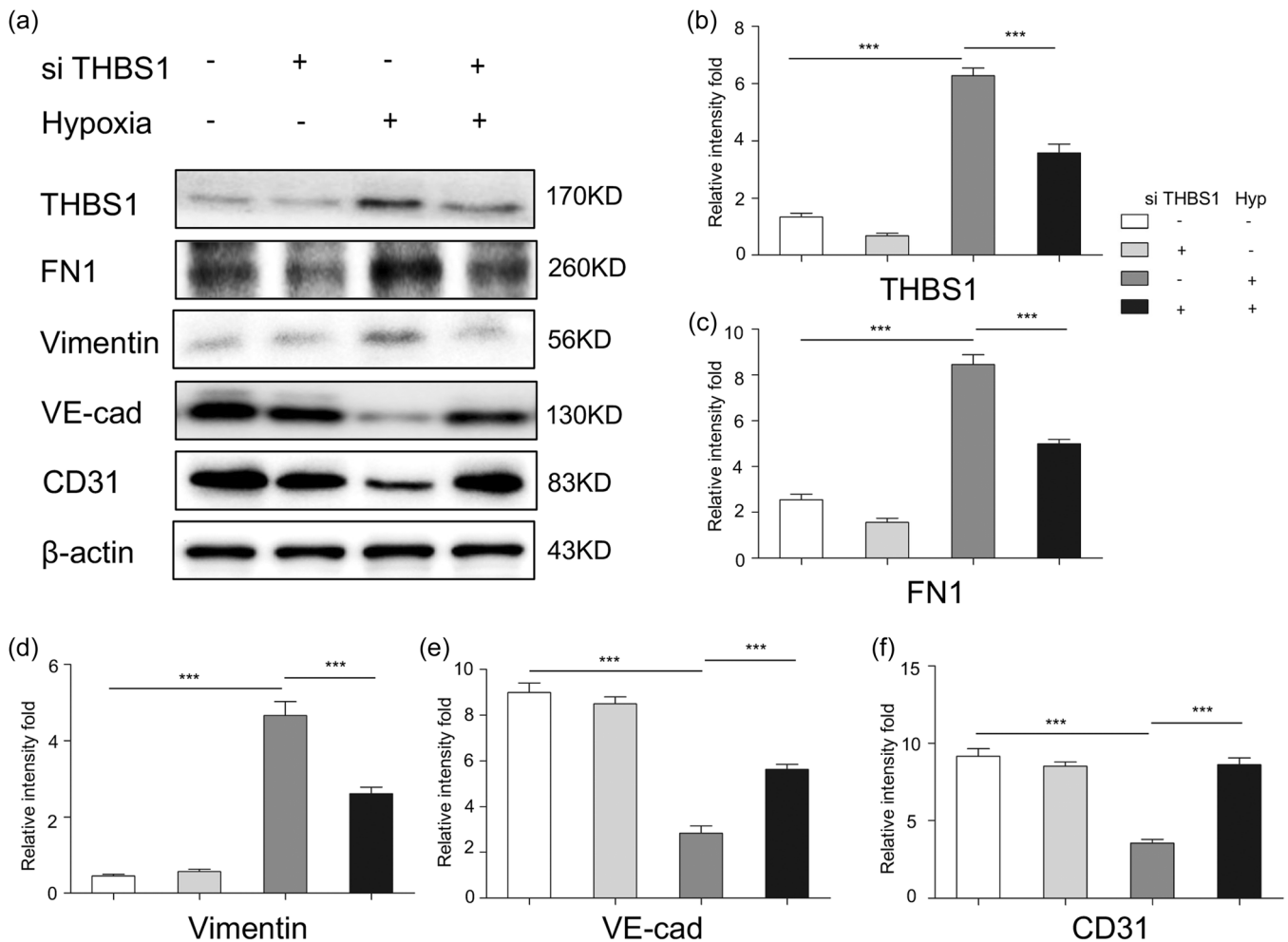
FIGURE 5 Knockdown of THBS1 attenuates hypoxia induced EndMT in human pulmonary artery endothelial cells (HPAEC). (a) Western blot analysis shows THBS1 (Thrombospondin 1), FN (fibronectin) 1, CD31, VE (vascular endothelial)-cadherin, and vimentin protein expression levels in hypoxia-induced HPAEC. (b–f) Graphs show the quantification of THBS1, FN1, CD31, VE-cad, and vimentin protein expression levels normalized by β-actin protein expression measured from hypoxia-induced HPAEC. Error bars represent means ± SEM ($n = 6$ in each group). *$p < 0.05$, **$p < 0.01$, and ***$p < 0.001$. si THBS1, knockdown of THBS1; VE-cad, VE-cadherin.

PH mice.[31] It was also reported that THBS1 activates TGF-β1 in the development of bronchopulmonary dysplasia (BPD).[32] Furthermore, THBS1 was reported to be regulated by HIF-2α in hypoxia-driven vascular remodeling of PH[20] while endothelial HIF-2α contributed to severe PH due to EndMT, suggesting that THBS1 may involve in hypoxia induced EndMT via HIF-2α which need to further explore in further.

In conclusion, our work demonstrated that THBS1 was involved in hypoxic pulmonary vascular remodeling of PH via EndMT, and this discovery could have therapeutic implications for PH. Additional research is necessary to delve into the detailed mechanisms of THBS1, which may work as a critical molecular player of EndMT in PH, will provide a new insight of research in the pathophysiology of PH.

AUTHOR CONTRIBUTIONS

Bingming Peng designed the study, collected specimens, analyzed and interpreted the data, wrote the manuscript, performed data analysis, and revised the manuscript. Yingzhen Zhou and Xingmeng Fu contributed to the provision of specimens and interpretation of data. Li Chen, Zhengxia Pan, Qijian Yi, and Tengteng Zhao designed the study and revised the manuscript. Ting Wang contributed to the study design, provided financial support, performed data analysis and interpretation, wrote, edited, and revised the manuscript, and provided final approval.

Chongqing Postdoctoral International Exchange Training Program (2021JLPY001), and National Clinical Medical Research Center (NCRC-2022-GP-08).

CONFLICT OF INTEREST STATEMENT

DATA AVAILABILITY STATEMENT

The transcriptome Sequence data associated with this project are available from the NCBI Sequence Read Archive (SRA) database with accession number PRJNA1181134.

ETHICS STATEMENT

All animal studies were approved by the Ethics Committee of the University of California, San Diego (La Jolla, CA) and executed according to the IACUC guidelines.

ORCID

Ting Wang https://orcid.org/0000-0001-5512-8026

REFERENCES

1. O'Callaghan DS, Savale L, Montani D, Jaïs X, Sitbon O, Simonneau G, Humbert M. Treatment of pulmonary arterial hypertension with targeted therapies. Nat Rev Cardiol. 2011;8(9):526–38.

2. Humbert M, Kovacs G, Hoeper MM, Badagliacca R, Berger RMF, Brida M, Carlsen J, Coats AJS, Escribano-Subias P, Ferrari P, Ferreira DS, Ghofrani HA, Giannakoulas G, Kiely DG, Mayer E, Meszaros G, Nagavci B, Olsson KM, Pepke-Zaba J, Quint JK, Radegran G, Simonneau G, Sitbon O, Tonia T, Toshner M, Vachiery JL, Noordegraaf AV, Delcroix M, Rosenkranz S. 2022 ESC/ERS Guidelines for the diagnosis and treatment of pulmonary hypertension. G Ital Cardiol. 2023;24(4):1e-116e.

3. Egito ESET, Aiello VD, Bosisio IBJ, Lichtenfels AJ, Horta ALM, Saldiva PHN, Capelozzi VL. Vascular remodeling process in reversibility of pulmonary arterial hypertension secondary to congenital heart disease. Pathol Res Pract. 2003;199(8):521–32.

4. Zhang B, Niu W, Dong HY, Liu ML, Luo Y, Li ZC. Hypoxia induces endothelial-mesenchymal transition in pulmonary vascular remodeling. Int J Mol Med. 2018;42(1):270–8.

5. Ranchoux B, Antigny F, Rucker-Martin C, Hautefort A, Péchoux C, Bogaard HJ, Dorfmüller P, Remy S, Lecerf F, Planté S, Chat S, Fadel E, Houssaini A, Anegon I, Adnot S, Simonneau G, Humbert M, Cohen-Kaminsky S, Perros F. Endothelial-to-mesenchymal transition in pulmonary hypertension. Circulation. 2015;131(11):1006–18.

6. Arciniegas E, Frid MG, Douglas IS, Stenmark KR. Perspectives on endothelial-to-mesenchymal transition: potential contribution to vascular remodeling in chronic pulmonary hypertension. Am J Physiol Lung Cell Mol Physiol. 2007;293(1):L1–8.

7. Gorelova A, Berman M, Al Ghouleh I. Endothelial-to-mesenchymal transition in pulmonary arterial hypertension. Antioxid Redox Signaling. 2021;34(12):891–914.

8. Frid MG, Kale VA, Stenmark KR. Mature vascular endothelium can give rise to smooth muscle cells via endothelial-mesenchymal transdifferentiation: in vitro analysis. Circ Res. 2002;90(11):1189–96.

9. Wang JJ, Chong QY, Sun XB, You ML, Pandey V, Chen YJ, Zhuang QS, Liu DX, Ma L, Wu ZS, Zhu T, Lobie PE. Autocrine hGH stimulates oncogenicity, epithelial-mesenchymal transition and cancer stem cell-like behavior in human colorectal carcinoma. Oncotarget. 2017;8(61):103900–18.

10. Blanchard N, Link PA, Farkas D, Harmon B, Hudson J, Bogamuwa S, Piper B, Authelet K, Cool CD, Heise RL, Freishtat R, Farkas L. Dichotomous role of integrin-β5 in lung endothelial cells. Pulm Circ. 2022;12(4):e12156.

11. Wang LL, Zhu XL, Han SH, Xu L. Hypoxia upregulates NOTCH3 signaling pathway to promote endothelial-mesenchymal transition in pulmonary artery endothelial cells. Evid Based Complement Alternat Med. 2021;2021:1525619.

12. Wei X, Wumaier G, Zhu N, Dong L, Li C, Xia J, Zhang Y, Zhang P, Zhang X, Zhang Y, Li S. Protein tyrosine phosphatase L1 represses endothelial-mesenchymal transition by inhibiting IL-1β/NF-κB/Snail signaling. Acta Pharmacol Sin. 2020;41(8):1102–10.

13. Peixoto P, Etcheverry A, Aubry M, Missey A, Lachat C, Perrard J, Hendrick E, Delage-Mourroux R, Mosser J, Borg C, Feugeas JP, Herfs M, Boyer-Guittaut M, Hervouet E. EMT is associated with an epigenetic signature of ECM remodeling genes. Cell Death Dis. 2019;10(3):205.

14. Huang J, Lu W, Ouyang H, Chen Y, Zhang C, Luo X, Li M, Shu J, Zheng Q, Chen H, Chen J, Tang H, Sun D, Yuan JXJ, Yang K, Wang J. Transplantation of mesenchymal stem cells attenuates pulmonary hypertension by normalizing the endothelial-to-mesenchymal transition. Am J Respir Cell Mol Biol. 2020;62(1):49–60.

15. Adams JC. Thrombospondin-1. Int J Biochem Cell Biol. 1997;29(6):861–5.

16. Bauer PM, Bauer EM, Rogers NM, Yao M, Feijoo-Cuaresma M, Pilewski JM, Champion HC, Zuckerbraun BS, Calzada MJ, Isenberg JS. Activated CD47 promotes pulmonary arterial hypertension through targeting caveolin-1. Cardiovasc Res. 2012;93(4):682–93.

17. Ochoa CD, Yu L, Al-Ansari E, Hales CA, Quinn DA. Thrombospondin-1 null mice are resistant to hypoxia-induced pulmonary hypertension. J Cardiothorac Surg. 2010;5:32.

18. Isenberg JS, Hyodo F, Matsumoto KI, Romeo MJ, Abu-Asab M, Tsokos M, Kuppusamy P, Wink DA, Krishna MC, Roberts DD. Thrombospondin-1 limits ischemic tissue survival by inhibiting nitric oxide-mediated vascular smooth muscle relaxation. Blood. 2007;109(5):1945–52.

19. Isenberg JS, Qin Y, Maxhimer JB, Sipes JM, Despres D, Schnermann J, Frazier WA, Roberts DD. Thrombospondin-1 and CD47 regulate blood pressure and cardiac responses to vasoactive stress. Matrix Biol. 2009;28(2):110–9.

20. Labrousse-Arias D, Castillo-González R, Rogers NM, Torres-Capelli M, Barreira B, Aragonés J, Cogolludo Á, Isenberg JS, Calzada MJ. HIF-2α-mediated induction of pulmonary thrombospondin-1 contributes to hypoxia-driven vascular remodelling and vasoconstriction. Cardiovasc Res. 2016;109(1):115–30.

21. Chemla D, Castelain V, Humbert M, Hébert JL, Simonneau G, Lecarpentier Y, Hervé P. New formula for predicting mean pulmonary artery pressure using systolic pulmonary artery pressure. Chest. 2004;126(4):1313–7.

22. Parasuraman S, Walker S, Loudon BL, Gollop ND, Wilson AM, Lowery C, Frenneaux MP. Assessment of pulmonary artery pressure by echocardiography—a comprehensive review. Int J Cardiol Heart Vasc. 2016;12:45–51.

23. Sun X, Perl AK, Li R, Bell SM, Sajti E, Kalinichenko VV, Kalin TV, Misra RS, Deshmukh H, Clair G, Kyle J, Crotty Alexander LE, Masso-Silva JA, Kitzmiller JA, Wikenheiser-Brokamp KA, Deutsch G, Guo M, Du Y, Morley MP, Valdez MJ, Yu HV, Jin K, Bardes EE, Zepp JA, Neithamer T, Basil MC, Zacharias WJ, Verheyden J, Young R, Bandyopadhyay G, Lin S, Ansong C, Adkins J, Salomonis N, Aronow BJ, Xu Y, Pryhuber G, Whitsett J, Morrisey EE. A census of the lung: CellCards from LungMAP. Dev Cell. 2022;57(1):112–45.

24. Hansmann G, Koestenberger M, Alastalo TP, Apitz C, Austin ED, Bonnet D, Budts W, D'Alto M, Gatzoulis MA, Hasan BS, Kozlik-Feldmann R, Kumar RK, Lammers AE, Latus H, Michel-Behnke I, Miera O, Morrell NW, Pieles G, Quandt D, Sallmon H, Schranz D, Tran-Lundmark K, Tulloh RMR, Warnecke G, Wåhlander H, Weber SC, Zartner P. 2019 updated consensus statement on the diagnosis and treatment of pediatric pulmonary hypertension: The European Pediatric Pulmonary Vascular Disease Network (EPPVDN), endorsed by AEPC, ESPR and ISHLT. J Heart Lung Transplant. 2019;38(9):879–901.

25. Tang H, Babicheva A, McDermott KM, Gu Y, Ayon RJ, Song S, Wang Z, Gupta A, Zhou T, Sun X, Dash S, Wang Z, Balistrieri A, Zheng Q, Cordery AG, Desai AA, Rischard F, Khalpey Z, Wang J, Black SM, Garcia JGN, Makino A, Yuan JX. Endothelial HIF-2alpha contributes to severe pulmonary hypertension due to endothelial-to-mesenchymal transition. Am J Physiol Lung Cell Mol Physiol. 2018;314(2):L256–75.

26. Murphy-Ullrich JE, Suto MJ. Thrombospondin-1 regulation of latent TGF-β activation: a therapeutic target for fibrotic disease. Matrix Biol. 2018;68–69:28–43.

27. Imamori M, Hosooka T, Imi Y, Hosokawa Y, Yamaguchi K, Itoh Y, Ogawa W. Thrombospondin-1 promotes liver fibrosis by enhancing TGF-beta action in hepatic stellate cells. Biochem Biophys Res Commun. 2024;693:149369.

28. Lu A, Pallero MA, Lei W, Hong H, Yang Y, Suto MJ, Murphy-Ullrich JE. Inhibition of transforming growth factor-β activation diminishes tumor progression and osteolytic bone disease in mouse models of multiple myeloma. Am J Pathol. 2016;186(3):678–90.

29. Song S, Shi C, Bian Y, Yang Z, Mu L, Wu H, Duan H, Shi Y. Sestrin2 remedies podocyte injury via orchestrating TSP-1/TGF-β1/Smad3 axis in diabetic kidney disease. Cell Death Dis. 2022;13(7):663.

30. Enright MF, Welch BL, Newman R, Perry BM. The hospital: psychology's challenge in the 1990's. Am Psychol. 1990;45(9):1057–8.

31. Kumar R, Mickael C, Kassa B, Sanders L, Hernandez-Saavedra D, Koyanagi DE, Kumar S, Pugliese SC, Thomas S, McClendon J, Maloney JP, Janssen WJ, Stenmark KR, Tuder RM, Graham BB. Interstitial macrophage-derived thrombospondin-1 contributes to hypoxia-induced pulmonary hypertension. Cardiovasc Res. 2020;116(12):2021–30.

32. Ruschkowski BA, Esmaeil Y, Daniel K, Gaudet C, Yeganeh B, Grynspan D, Jankov RP. Thrombospondin-1 plays a major pathogenic role in experimental and human broncho-pulmonary dysplasia. Am J Respir Crit Care Med. 2022;205(6):685–99.

SUPPORTING INFORMATION

Additional supporting information can be found online in the Supporting Information section at the end of this article.